

Modeling differential diffusion in non-premixed combustion: soot transport in the mixture fraction coordinate

By J. C. Hewson[†], D. O. Lignell[‡] AND A. R. Kerstein[‡]

An *a priori* analysis of a recent formulation of the conditional-moment-closure (CMC) model is carried out using results of a 3-D direct numerical simulation (DNS) with reduced ethylene chemistry and a simplified soot model. Of particular interest is a term that is new in the recent CMC formulation. This term is associated with the role that differential diffusion plays in transporting soot relative to the mixture fraction coordinate. In particular, it describes the role of small-scale diffusive processes on that transport, and it has been modeled using an eddy-diffusivity approximation. The results suggest that the eddy-diffusivity approximation works well over a wide range of conditions for soot, but that the approximation, in the present form, breaks down for species for which the flame chemistry is fast, such as those participating in the main-flame chemistry. This breakdown is analyzed in a way that suggests a correction to the eddy-diffusivity model for fast chemistry, but this correction has not been carried out at this point.

1. Introduction

The evolution of soot in non-premixed flames is of significant importance because of its role in radiative heat transfer and the significant health consequences of emitted soot as a pollutant. Among the many complexities of predicting turbulent reacting flows in general, predictions of soot evolution present several particular challenges. One of these challenges is related to the substantial difference in the diffusivity of soot particles relative to the other reacting gases. This work focuses on this issue, generally referred to as differential diffusion, and seeks to understand how differential diffusion affects the local stoichiometry and temperature of the soot particles. This is significant because the chemical evolution of soot particles is a strong function of the temperature and stoichiometry. The temperature-stoichiometry relationship is also important because of the role that soot plays in radiative heat transfer. In sooting flames, the primary source of radiant heat flux is thermal emissions from soot while the primary in-fire sink for radiant flux is also soot. Radiant heat flux is then a function of the joint soot-temperature distribution.

In turbulent fires, knowledge of the joint soot-temperature probability density function (pdf) is not readily obtained. One class of approaches that can be used to approximate this quantity is the conserved-scalar modeling approach. This approach is based on the idea that the thermochemical state can be referenced to a reduced set of variables for which the pdf is easier to predict. In non-premixed combustion, this reduced variable is the mixture fraction, the fraction of the local mixture that originated from the fuel source. If the pdf of the mixture fraction can be obtained and if the temperature and soot

[†] Fire and Aerosol Science, Sandia National Laboratories, Albuquerque, NM

[‡] Combustion Research Facility, Sandia National Laboratories, Livermore, CA

can be obtained as a function of the mixture fraction, then the joint soot-temperature pdf is obtained.

The growth of soot particles generally occurs at a rate that is slow relative to the main flame chemistry and characteristics of the soot distribution typically evolve over the scales of the entire turbulent flame. This necessitates a treatment that includes the flame-scale evolution of the soot if one seeks to predict the behavior of soot. There are two general frameworks for developing conserved-scalar modeling approaches that allow the evolution of flame-scale quantities: conditional-moment closure (CMC) (Klimenko & Bilger 1999) and unsteady-laminar flamelet models (ULFM) (Pitsch *et al.* 1998). In the limit in which all of the transport coefficients are equal, both approaches are relatively straightforward and have been employed successfully in many studies. When species diffusivities differ, additional complications arise in the formulation. A model for flamelets with full differential diffusion has been derived by Pitsch & Peters (1998), but in the application to jet flames the best agreement with scalar fields was obtained by switching from full differential diffusion to unity Lewis numbers at the end of the jet potential core (Pitsch *et al.* 1998). For CMC, Kronenburg & Bilger (1997) developed a model to account for the effects of differential diffusion based on the analysis of direct numerical simulations (DNS). This model retains the different diffusivities of the species, but provides a term that tends to move species profiles closer to that which would be obtained with equal diffusivities as observed in their DNS; evaluation of this term requires the solution of additional transport equations for each differentially diffusing scalar. For flames with soot in which differential diffusion is important, results have been reported by both Pitsch *et al.* (2000) and Kronenburg & Bilger (2000). Recently, Hewson *et al.* (2006) proposed another model in the CMC context to describe the effects of differential diffusion on soot evolution in one-dimensional turbulence (ODT) simulations (Ricks *et al.* 2008). This model does not require the solution of an additional transport equation and further explains the transition to unity Lewis numbers observed by Pitsch *et al.* (1998). This model has also been evaluated using DNS results in Lignell *et al.* (2008*a*) where it was confirmed that the model works well when applied in an *a priori* sense to soot evolution.

Here, we reexamine this recent differential-diffusion model of Hewson *et al.* (2006) in an effort to understand the degree of universality that this model might exhibit. The model will be examined using the same DNS results from Lignell *et al.* (2008*a*). The DNS methods are described briefly in the following section. In Sec. 3 the recent derivation of the CMC equations is provided in brief because it gives a somewhat different form of the equations. The proposed model is also introduced there. Finally, in Sec. 4 the model is evaluated in the context of the DNS results for both soot and other reacting scalars.

2. Direct numerical simulations

Results of a direct numerical simulation of a non-premixed planar ethylene jet flame with soot formation and transport are used in the analysis of the conditional-moment models under consideration. This simulation is presented in Lignell *et al.* (2008*b*, 2008*a*). Here, a brief code description and summary of the simulation configuration are presented.

The simulation was performed using the S3D code developed at Sandia National Laboratories. S3D solves the compressible, reacting Navier-Stokes equations using an explicit, fourth-order Runge-Kutta integration scheme and eighth-order central-difference discretization operators with a tenth-order spatial filter. A Cartesian computational grid is used with domain decomposition using MPI for parallelization. Composition and

temperature-dependent thermodynamic and transport properties are evaluated using Chemkin. A reduced, 19 species, 167 reaction ethylene mechanism was evolved using the standard conservation equation

$$\frac{\partial \rho Y_i}{\partial t} + \nabla \cdot (\rho Y_i \vec{v}) = -\nabla \cdot (\rho D_i \nabla Y_i) + \rho w_i \quad (2.1)$$

to represent the combustion system. Here ρ is the density, Y_i is the species mass fraction, \vec{v} is the bulk flow velocity, D_i is the species diffusion coefficient and w_i is the chemical source term. Soot formation and transport is computed using the method of moments. The first three mass moments of the particle size distribution are transported using the following transport equations:

$$\begin{aligned} \frac{\partial n}{\partial t} + \nabla \cdot (n \vec{v}) &= -\nabla \cdot (n \vec{v}_{thm}) + \rho w_n, \\ \frac{\partial \rho Y_s}{\partial t} + \nabla \cdot (\rho Y_s \vec{v}) &= -\nabla \cdot (\rho Y_s \vec{v}_{thm}) + \rho w_{\rho Y_s}, \\ \frac{\partial M_2}{\partial t} + \nabla \cdot (M_2 \vec{v}) &= -\nabla \cdot (M_2 \vec{v}_{thm}) + \rho w_{M_2}. \end{aligned} \quad (2.2)$$

Here, \vec{v}_{thm} is the thermophoretic diffusion velocity, and n , ρY_s and M_2 are the soot mass moments with source terms w . The effective Brownian diffusion coefficient of soot is negligibly small. Soot particles are assumed spherical and an assumed shape lognormal size distribution is used to close the moment source terms. The soot reaction model is based on the model of Leung *et al.* (1991) and consists of nucleation, coagulation, growth and oxidation steps.

The simulation configuration consists of a planar, temporally evolving ethylene jet with periodic boundaries in the streamwise and spanwise directions, and non-reflecting outflow boundaries in the cross-stream direction. Combustion occurs at 1 atm between a central fuel core of ethylene and nitrogen surrounded by oxidizer. The streams flow in opposite directions, are both preheated to 550 K, and consist of fuel and air with nitrogen transferred from the air stream to the fuel stream to give a stoichiometric mixture fraction of 0.25. A steady laminar flamelet solution was used to initialize the composition and isotropic turbulence was overlaid in the jet core to trip the shear layers. The jet Reynolds number is 3700, and the simulation is run for 50 characteristic jet times.

Figure 1 shows a planar slice through the spanwise direction of contours of OH mass fraction (lines) along with filled and smoothed contours of soot mass fraction at 41 jet times (τ_j). Soot initially forms on the fuel side of the flame surface at $\xi = 0.4$. The low diffusivity of soot results in its being convected into the fuel core where it is strained and mixed with fuel and combustion products. The OH mass fraction, along with temperature, and other gaseous species are significantly more diffuse than the corresponding soot mass fraction as evident in the figure. The high diffusivity of gaseous species relative to soot results in strong differential diffusion between soot and the gaseous mixture fraction. Figure 2 shows profiles of mixture fraction, CO mass fraction and soot mass fraction along a typical vertical (cross-stream) line of sight through the domain at $50\tau_j$. The global CO structure is qualitatively similar to that of the mixture fraction. In contrast, the fine structure of the soot mass fraction shows significant variability across a given monotonic region of the mixture-fraction profile.

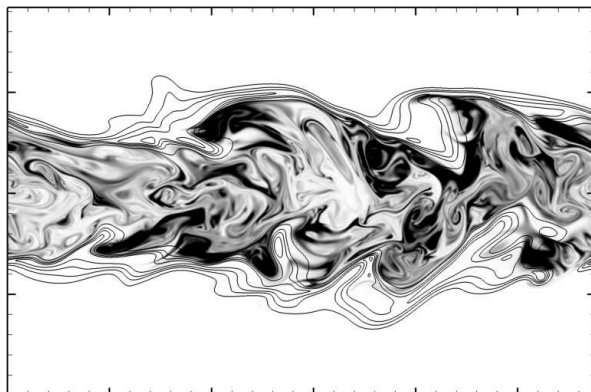


FIGURE 1. Contours of OH mass fraction (lines): five contours spaced from 0.0005 to 0.007, and grayscale soot mass fraction with range 0 (white) to 0.00005 (black) at $41\tau_j$.

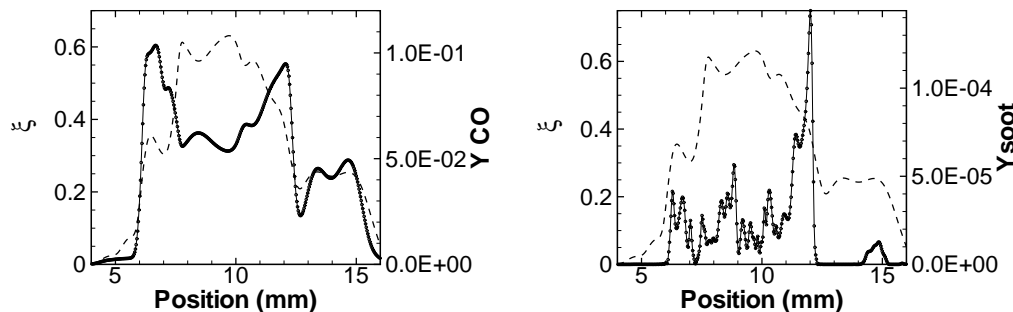


FIGURE 2. Instantaneous profiles along a line of sight through the cross-stream direction at $50\tau_j$ with mixture fraction (dashed), CO mass fraction (left panel, lines and symbols) and soot mass fraction (right panel, lines and symbols).

3. The conditional-moment equation and a closure hypothesis

There are two basic approaches to deriving the CMC equations. The method proposed originally by Bilger (1993), decomposing the variables into conditional means and fluctuations, was employed by Kronenburg & Bilger (1997) to analyze differential diffusion and then to study soot evolution in jet flames (Kronenburg *et al.* 2000). In Hewson *et al.* (2006) and Lignell *et al.* (2008a), the conditional-moment equations were derived in a manner analogous to the method of Klimenko (1990) that is based on the joint-pdf evolution equation. There are two significant differences between the original CMC derivations by Klimenko (1990) and the derivations in Hewson *et al.* (2006) and Lignell *et al.* (2008a). In the latter cases, the equal diffusivity assumption was relaxed, resulting in some different terms appearing in the conditional-moment equations. Also, the closure assumptions employed by Klimenko were relaxed to allow for the effect of conditional fluctuations to contribute to the transport of scalars in the mixture-fraction coordinate. In this section, the alternate derivations are reviewed including the suggested closure models. Of particular interest is the model for a term involving the conditional fluctuations. The model for this term will be discussed in Sec. 4.

The derivation starts with the joint-pdf equation that is obtained in a standard manner using the conservation equations for the scalar of interest, either the species in Eq. (2.1)

or the soot moments in Eq. (2.2) and the mixture fraction, ξ . Klimenko & Bilger (1999) provide an exposition for the equal-diffusivity, variable-density and inhomogeneous-flow case from which the mechanistic details can be obtained. Here, only the spatially homogeneous limit is considered and the terms that are small at high Reynolds numbers are ignored (Klimenko & Bilger 1999). Also neglected here are the thermophoretic contributions to soot transport that were also shown to be less significant (Lignell *et al.*, 2008a). For reference, the equations with these terms retained are available in Hewson *et al.* (2006) and Lignell *et al.* (2008a). The conditional-moment equation for a scalar Y_i is obtained from the joint pdf by multiplying by Y_i and integrating across all variables of the joint pdf except for the mixture fraction

$$\begin{aligned} \frac{\partial \langle \rho Y_i | \eta \rangle f_\xi}{\partial t} &= \langle \rho w_i | \eta \rangle f_\xi \\ &- \frac{\partial^2}{\partial \eta^2} [\langle \rho D_i (\nabla \xi)^2 Y_i | \eta \rangle f_\xi] \\ &+ \frac{\partial}{\partial \eta} [\langle 2\rho D_i (\nabla Y_i \nabla \xi) | \eta \rangle f_\xi] \\ &- \frac{\partial}{\partial \eta} (\langle \nabla \cdot [\rho (D_\xi - D_i) \nabla \xi] Y_i | \eta \rangle f_\xi), \end{aligned} \quad (3.1)$$

where the notation $\langle \cdot | \eta \rangle$ indicates conditional averaging with the sample-space variable η and f_ξ is the marginal pdf for the mixture fraction. The terms on the right-hand side (r.h.s.) represent the conditional averages of contributions from the chemical source term, the product of the dissipation and Y_i , the ξ - Y_i cross-dissipation and the differential diffusion. This differs from the derivation in Klimenko & Bilger (1999) in that the diffusivity of the scalar, D_i , appears in most of the terms; also, the differential diffusion contribution takes a somewhat different form.

Up to this point, Eq. (3.1) is an exact equation. As is typical in turbulence modeling, a useful form of the equation requires some modeling assumptions. The conditional averages of density, Y_i , the scalar-dissipation rate and the diffusion velocity are defined for convenience

$$\rho_\eta = \langle \rho | \eta \rangle, \quad Q_i = \frac{\langle \rho Y_i | \eta \rangle}{\rho_\eta}, \quad \chi_\eta = \frac{\langle 2\rho D_\xi (\nabla \xi)^2 | \eta \rangle}{\rho_\eta}, \quad M_\eta = \frac{\langle \nabla \cdot (\rho D_\xi \nabla \xi) | \eta \rangle}{\rho_\eta}. \quad (3.2)$$

For the second and third terms of Eq. (3.1) on the r.h.s., Klimenko & Bilger (1999) suggest the closures

$$\langle \rho D_i (\nabla \xi)^2 Y_i | \eta \rangle \approx \frac{\rho_\eta \chi_\eta Q_i}{2Le_i}, \quad \langle 2\rho D_i (\nabla Y_i \nabla \xi) | \eta \rangle \approx \frac{\rho_\eta \chi_\eta}{Le_i} \frac{\partial Q_i}{\partial \eta}. \quad (3.3)$$

The first of these is exact if there is no correlation between the dissipation and the scalar while the second is exact if the scalar gradient is perfectly correlated with the mixture-fraction gradient by $\nabla \xi = \nabla Y_i \partial Q_i / \partial \eta$. Prior analysis of these closure approximations shows that the separate approximations are often not very good, but the combined closure (as proposed by Klimenko) is substantially better (Hewson *et al.* 2006). The current work focuses on the analogous approximations for the fourth term,

$$\langle \nabla \cdot [\rho (D_\xi - D_i) \nabla \xi] Y_i | \eta \rangle \approx \left(1 - \frac{1}{Le_i}\right) \rho_\eta M_\eta Q_i. \quad (3.4)$$

It was found in previous work that this approximation is particularly poor for soot

(Hewson *et al.* 2006), and a residual fluctuation contribution was retained. The residual fluctuation is expressed in terms of the conditional fluctuations for Y_i and for the diffusion velocity

$$y'_i = \frac{\rho Y_i - \rho_\eta Q_i}{\rho_\eta}, \quad M' = \frac{\nabla \cdot (\rho D_\xi \nabla \xi) - \rho_\eta M_\eta}{\rho_\eta}. \quad (3.5)$$

With the decomposition suggested in Eq. (3.5), the fourth term on the r.h.s. of Eq. (3.1) is

$$\begin{aligned} -\frac{\partial}{\partial \eta} (\langle \nabla \cdot [\rho(D_\xi - D_i)\nabla \xi] Y_i | \eta \rangle f_\xi) &= -\left(1 - \frac{1}{Le_i}\right) \frac{\partial}{\partial \eta} (\rho_\eta M_\eta Q_i f_\xi) \\ &\quad - \left(1 - \frac{1}{Le_i}\right) \frac{\partial}{\partial \eta} (\rho_\eta \langle M' y'_i | \eta \rangle f_\xi). \end{aligned} \quad (3.6)$$

While the retention of conditional fluctuations in the mixture-fraction transport terms of the CMC equations has generally been neglected for the first-order moments, Kim (2002) indicated that the terms of this form need to be retained to balance the equation for the derivation of the second-order CMC equations. Kim (2002) has also shown that this type of contribution is a significant contributor to the flux in the second-order CMC equations. The first term on the r.h.s. of Eq. (3.6) is more easily represented in terms of the scalar-dissipation rate by using the mathematical identity

$$\frac{\partial}{\partial \eta} (\rho_\eta M_\eta f_\xi) = \frac{\partial^2}{\partial \eta^2} \left(\frac{\rho_\eta \chi_\eta f_\xi}{2} \right) - \langle \nabla \cdot (\rho D_\xi \nabla f_\xi) | \eta \rangle, \quad (3.7)$$

and neglecting the last term, which is only important at low Reynolds numbers.

It is suggested (Hewson *et al.* 2006) that the last term in Eq. (3.6) be represented using the gradient transport assumption. This reasoning arises because M' is dimensionally a velocity fluctuation in the mixture-fraction coordinate, $\rho_\eta f_\xi$ is a density in the mixture-fraction coordinate and y'_i is a scalar fluctuation. Thus, this term looks like the turbulent scalar transport term, but in the mixture-fraction coordinate. In analogy to the closure of turbulent transport in physical space, we identify an “eddy diffusivity” in the mixture-fraction coordinate. To do so, consider the history of a fluid element. This fluid element is subject to mixture-fraction fluctuations on the diffusive (Batchelor) time scales of order $l_B |\nabla \xi|$ where l_B is the Batchelor scale for the mixture fraction. These fluctuations occur over time scales of t_B , the Batchelor time scale. A diffusivity formed from these quantities is $l_B^2 |\nabla \xi|^2 / t_B$. Since the Batchelor scales are related by D_ξ as $D_\xi \approx l_B^2 / t_B$ an estimate, good only to within an order of magnitude, of the diffusivity associated with mixture-fraction fluctuations is the scalar-dissipation rate. This leads to the approximation of the last term in Eq. (3.6) as

$$-\frac{\partial}{\partial \eta} (\rho_\eta \langle M' y'_i | \eta \rangle f_\xi) \approx \frac{\rho_\eta \chi_\eta f_\xi}{2 Le_{DD}} \frac{\partial^2 Q_i}{\partial \eta^2} \quad (3.8)$$

where a constant, Le_{DD} , has been added because the “eddy diffusivity” is only approximately represented by the scalar dissipation rate.

Applying the definitions in Eqs. (3.2) through (3.8) to Eq. (3.1) the CMC equation is

written, after some manipulation, as

$$\begin{aligned}
 \frac{\partial(\rho_\eta Q_i f_\xi)}{\partial t} &= \langle \rho w_i | \eta \rangle f_\xi \\
 &+ \frac{\rho_\eta \chi_\eta f_\xi}{2Le_i} \frac{\partial^2 Q_i}{\partial \eta^2} \\
 &- \frac{\partial^2}{\partial \eta^2} \left(\frac{\rho_\eta \chi_\eta f_\xi}{2} \right) Q_i \\
 &- \left(1 - \frac{1}{Le_i} \right) \frac{\partial}{\partial \eta} \left(\frac{\rho_\eta \chi_\eta f_\xi}{2} \right) \frac{\partial Q_i}{\partial \eta} \\
 &+ \left(1 - \frac{1}{Le_i} \right) \frac{\rho_\eta \chi_\eta f_\xi}{2Le_{DD}} \frac{\partial^2 Q_i}{\partial \eta^2}.
 \end{aligned} \tag{3.9}$$

This equation is in conservative form with the pdf, f_ξ , appearing in all of the terms in the role of the density in the mixture-fraction coordinate. In converting to non-conservative form, the mixture-fraction pdf-evolution equation multiplied by Q_i is subtracted from Eq. (3.9), eliminating the third term on the r.h.s. The first and second terms on the r.h.s. of Eq. (3.9) are the chemical source term and the typical transport in the mixture-fraction coordinate term associated with unity-Lewis-number diffusion. The fourth term describes the advection in the mixture-fraction coordinate associated with the evolution of the mixture-fraction pdf. This contribution related to differential diffusion is attributed to the long-time mean evolution of the mixture composition that would occur in laminar flows as well as in turbulent flows. The fifth term is new in the recent formulations (Hewson *et al.* 2006) and will be discussed extensively in the following section. This contribution is related to the small-scale random fluctuations in the local composition and is only valid in turbulent flows.

4. Results and discussion

In this section, previous results that lead to the current discussion are first reviewed. The first application of the formulation in Eq. (3.9) was to the evolution of soot using the ODT model (Hewson *et al.* 2006). For soot, Le_i appearing in the second term on the r.h.s. of Eq. (3.9) is large enough that the standard diffusive transport in the mixture-fraction coordinate (second term on r.h.s of Eq. (3.9)) is negligible. The two contributions related to differential diffusion were identified there to be substantial, however, and the model proposed in Eq. (3.8) for the fluctuation term coming from the $\langle M' y'_i | \eta \rangle$ contribution was first suggested. There it was also shown that the constant Le_{DD} appearing in this model is of order unity.

The fact that Le_{DD} is of order unity is interesting in the context of the larger understanding of differential diffusion. It has been observed that the turbulent mixing tends to reduce the effect of differential diffusion (c.f. Pitsch *et al.* 1998 and Barlow *et al.* 2000), in effect making the flow look more like the scalars have a unity Lewis number. The two differential diffusion terms in Eq. (3.9) have different roles. The fourth term on the r.h.s. tends to enhance the effects of differential diffusion and has the same character as the differential diffusion terms that would appear in the laminar flow equations (i.e., Pitsch & Peters 2008). The fifth term on the r.h.s. tends to dissipate any effects of differential diffusion, and the fact that Le_{DD} is of order unity suggests that this term captures the basic physics of the tendency toward unity Lewis numbers for scalars in turbulent flows.

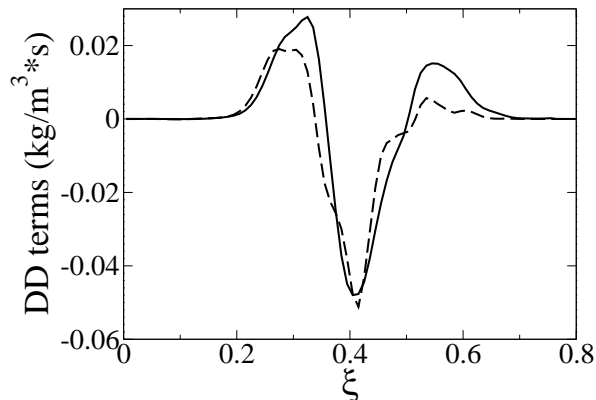


FIGURE 3. Differential diffusion associated with fluctuations (solid) and its model (dashed) from the left and right-hand sides of Eq. (3.8), respectively.

In Lignell *et al.* (2008a) the model was applied to the DNS described in Sec. 2. The results associated with soot transport there were in agreement with those in Hewson *et al.* (2006), and it was suggested that for soot $Le_{DD} = 3$. A comparison between the left and right-hand sides of Eq. (3.8) is shown in Fig. 3. This result also provides a reasonable fit to the earlier ODT data (Hewson *et al.* 2006). Of particular interest is the diversity of time and length scales in these two studies. In the ODT simulations, the Kolmogorov time scale was on the order of 1 ms while the Kolmogorov time scale was on the order of 50 μ s for the DNS. The mean scalar-dissipation rates in the ODT simulations were in the 0.1 - 1.0 s^{-1} range while those in the DNS were in the 10 - 100 s^{-1} range. This suggests some degree of universality in the value of Le_{DD} for soot.

However, when the model for the differential diffusion terms in Eq. (3.8) was applied to other species that comprise the main flame chemistry in the DNS (Lignell *et al.* 2008a), it was found to not be suitable, at least not for the same range of Le_{DD} . In some cases it was suggested that $Le_{DD} \gg 1$. In the present work, this observed behavior is discussed. To understand this behavior, it is helpful to follow the development of the eddy-diffusivity approximation. The eddy-diffusivity approximation arises from the analysis of a production-dissipation balance in the scalar fluctuation equation. As Peters (2000) shows (c.f. Sec. 1.8 of that book) chemical reactions with sufficiently large Damköhler numbers can alter the production-dissipation balance. Peters analyzed a model problem presented originally by Corrsin (1961) and showed that the scalar-flux term was reduced for a reaction that tended to reduce scalar fluctuations if the Damköhler number for that reaction was not small. To follow the reasoning in Peters, an estimate for the covariance of the reaction and scalar fluctuations is required. It is expected that reactions characterized by fast chemistry fall into the category examined by Corrsin since Q_i should describe a quasi-steady state that reactions should pull perturbations toward. For these cases, the approximation $\langle w'_i y'_i | \eta \rangle \approx -B_\eta \langle (y'_i)^2 | \eta \rangle$ is made. This approximation would not be accurate in all cases, especially for soot growth where a positive correlation is expected (more soot mass has greater surface area available for growth). However, since the Damköhler numbers, B_η/χ_η , for soot reactions are small, the chemical-source contribution to the scalar flux can be neglected. Following Peters (2000), an estimate for the

scalar flux, here in the mixture-fraction coordinate, is

$$\langle M' y'_i | \eta \rangle \approx \frac{\chi_\eta \rho_c^2}{1 + B_\eta / \chi_\eta} \frac{\partial Q_i}{\partial \eta}. \quad (4.1)$$

Here the correlation coefficient between M' and y' , ρ_c , has been introduced. Comparing this with Eq. (3.8) suggests that

$$\frac{1}{Le_{DD}} \approx \frac{\rho_c^2}{1 + B_\eta / \chi_\eta}. \quad (4.2)$$

There are two primary quantities that can affect the effective Lewis number for the $\langle M' y'_i | \eta \rangle$ scalar flux. A lack of correlation between the fluctuations M' and y'_i and fast chemistry (a large Damköhler number) both tend to increase Le_{DD} . As discussed by Corrsin (1961), the role of fast chemistry of the nature described by $\langle w'_i y'_i | \eta \rangle \approx -B_\eta \langle (y'_i)^2 | \eta \rangle$ is to reduce the magnitude of the scalar fluctuations. In Fig. 4, the quantities $\langle MY_i | \eta \rangle$ and $M_\eta Q_i$ are plotted, the difference between these being $\langle M' y'_i | \eta \rangle$. In this manner, it is possible to observe the conditions where the scalar flux associated with the fluctuations is significant relative to that associated with the mean evolution, $\langle MY_i | \eta \rangle$. Also plotted in Fig. 4 are the conditional means and fluctuations of the scalars. Results for three scalars are shown in Fig. 4: CO₂, H and soot, all of which should be affected to some degree by differential diffusion. It is seen that for CO₂, $\langle M' y'_{CO_2} | \eta \rangle \ll \langle MY_{CO_2} | \eta \rangle$. At the same time, $y'_{CO_2} \ll Q_{CO_2}$, and CO₂ is known to be close to partial equilibrium throughout the flame (i.e., the chemistry is fast). For the H atom $\langle M' y'_{CO_2} | \eta \rangle$ is small in the main flame zone but significant in the diffusive layers around the main flame zone following the behavior of y'_H compared with Q_H . In these layers, H is known to follow a reaction-diffusion balance and the reaction is not close to partial equilibrium (Hewson & Williams, 1999). For soot with its small Damköhler number, the magnitude of both $\langle M' y'_{CO_2} | \eta \rangle$ and y_s are substantial relative to the other terms, as has been noted (Hewson *et al.* 2006). While it would be desirable in the future to more directly evaluate the role of the Damköhler number to better understand Eqs. (4.1) and (4.2), the appropriate data is not available at this time. Overall, the trends suggest that the reduction in scalar fluctuations associated with fast chemistry is responsible for Le_{DD} being not of order unity for scalars in the main flame chemistry. Equations (4.1) and (4.2) do show that, given suitable information about the Damköhler number, it may be possible to identify the magnitude of the eddy-diffusivity contribution to differential diffusion as the Damköhler number increases, but this has not been pursued here.

The other parameter that appeared in Eq. (4.2) is the correlation coefficient. The correlation coefficients between M' and y'_i are plotted in Fig. 5 for the three scalars considered in Fig. 4. In Fig. 5 it is seen that the correlation coefficients in the regions of significance are of similar magnitude, being of order one-half. This suggests that there are no substantial differences in the applicability of Eq. (3.8) associated with a change in the degree of correlation between the diffusive term and the scalar fluctuation.

5. Conclusions

A recent formulation of the CMC equations has been examined using an *a priori* analysis with the results of a 3-D DNS using reduced ethylene chemistry and a simplified soot model. Of interest in the recent CMC formulation is a term modeling the effect of fine-scale differential diffusion, that associated with fluctuation of the diffusion velocity.

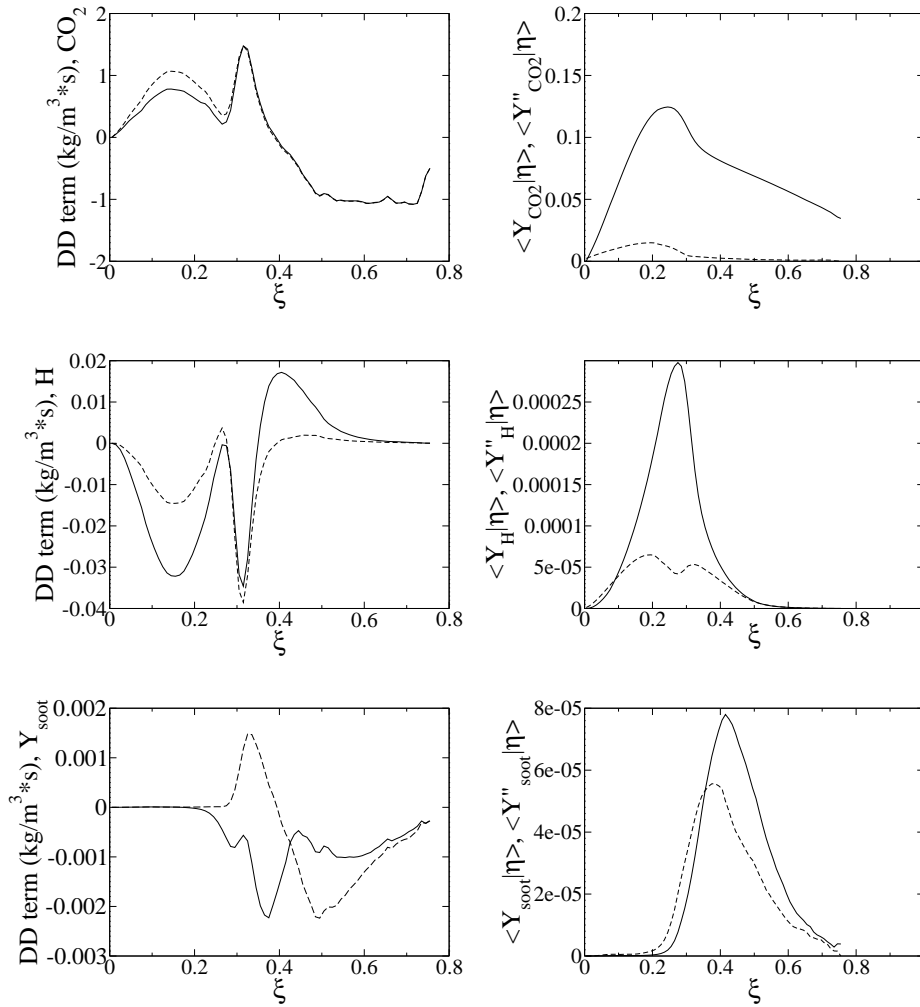


FIGURE 4. Conditional mean (solid) and standard deviations (dashed) of species mass fractions (right panels), and $\langle M_\eta Y_i | \eta \rangle$ (solid), $M_\eta Q_i$ (dashed) (left panels).

This term is modeled currently using an eddy-diffusivity approximation, but where the diffusivity is in the mixture-fraction coordinate and not the physical coordinate. For soot, this approximation has been shown to work well under a variety of conditions. For some species associated with the main-flame chemistry, this approximation is found to be less suitable. Results presented here suggest that the role of fast chemistry in reducing conditional scalar fluctuations are responsible for this change in behavior. That is, the eddy-diffusivity approximation is less suitable for systems with large Damköhler numbers, as has been noted elsewhere.

Acknowledgments

We are indebted to fellow Summer Program participants and the Center for Turbulence Research staff for their helpful suggestions, in particular to Seung Hyun Kim and

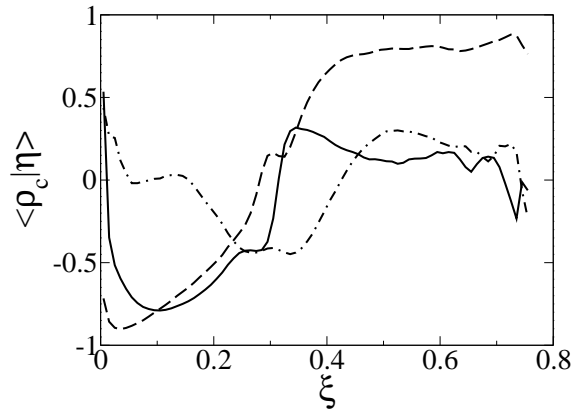


FIGURE 5. Conditional mean correlation coefficient between M_η and Y_i with species CO₂ (solid), H (dashed), soot (dash-dot) at $50\tau_j$.

Rodney Fox. Allen Ricks also provided many useful suggestions for this work. This work was conducted through support from Sandia National Laboratories, a multi-program laboratory operated by Sandia Corporation, a Lockheed Martin Company, for the United States Department of Energy's National Nuclear Security Administration under contract DE-AC04-94AL85000.

REFERENCES

- BARLOW, R. S., FIECHTNER, G. J., CARTER, C. D. & CHEN, J.-Y. 2000 Experiments on the scalar structure of turbulent CO/H₂/N₂ jet flames. *Combust. Flame* **120**, 549–569, also <http://www.ca.sandia.gov/tdf/DataArch/SANDchnWeb/SANDchn.html>.
- BILGER, R. W. 1993 Conditional moment closure for turbulent reacting flow. *Phys. Fluids A* **5**, 436.
- CORRSIN, S. 1961 The reactant concentration spectrum in turbulent mixing with a first-order reaction. *J. Fluid Mech.* **11**, 407–416.
- HEWSON, J. C., RICKS, A. J., TIESZEN, S. R., KERSTEIN, A. R. & FOX, R. O. 2006 Conditional-moment closure with differential diffusion for soot evolution in fire. In *Proceedings of the 2006 Summer Program*, pp. 311–323. Center for Turbulence Research, Stanford University.
- HEWSON, J. C. & WILLIAMS, F. A. 1999 Rate-ratio asymptotic analysis of methane-air diffusion flame structure for predicting production of oxides of nitrogen. *Combust. Flame* **117**, 441–476.
- KIM, S. H. 2002 On the conditional variance and covariance equations for second-order conditional moment closure. *Phys. Fluids* **16** (6), 2011–2014.
- KLIMENKO, A. Y. 1990 Multicomponent diffusion of various admixtures in turbulent flow. *Fluid Dynamics* **25**, 327–333.
- KLIMENKO, A. Y. & BILGER, R. W. 1999 Conditional moment closure for turbulent combustion. *Prog. Energy Combust. Sci.* **25**, 595–687.
- KRONENBURG, A. & BILGER, R. W. 1997 Modelling of differential diffusion in non-premixed nonreacting turbulent flows. *Phys. Fluids* **9** (5), 1435–1447.

- KRONENBURG, A., BILGER, R. W. & KENT, J. H. 2000 Modeling soot formation in turbulent methane-air jet diffusion flames. *Combust. Flame* **121**, 24–40.
- LEUNG, K. M., LINDSTEDT, R. P. & JONES, W. P. 1991 A simplified reaction mechanism for soot formation in nonpremixed flames. *Combust. Flame* **87**, 289–305.
- LIGNELL, D. O., CHEN, J. H. & SMITH, P. J. in press, 2008a Three-dimensional direct numerical simulation of soot formation and transport in a temporally evolving nonpremixed ethylene jet flame. *Combust. Flame* p. doi:10.1016/j.combustflame.2008.05.020. In press.
- LIGNELL, D. O., HEWSON, J. C. & CHEN, J. H. 2008b A-priori analysis of conditional moment closure modeling of a temporal ethylene jet flame with soot formation using direct numerical simulation. *Proc. Combust. Inst.* **32**, doi:10.1016/j.proci.2008.07.007. In press.
- PETERS, N. 2000 *Turbulent Combustion*. Cambridge University Press. Cambridge, United Kingdom.
- PITSCH, H., CHEN, M. & PETERS, N. 1998 Unsteady flamelet modeling of turbulent hydrogen/air diffusion flames. *Proc. Combust. Inst.* **27**, 1057–1064.
- PITSCH, H. & PETERS, N. 1998 A consistent flamelet formulation for non-premixed combustion considering differential diffusion effects. *Combust. Flame* **114**, 26–40.
- PITSCH, H., RIESMEIER, E. & PETERS, N. 2000 Unsteady flamelet modeling of soot formation in turbulent diffusion flames. *Combust. Sci. Tech.* **158**, 389–406.
- RICKS, A. J., HEWSON, J. C., KERSTEIN, A. R., GORE, J. P., TIESZEN, S. R. & ASHURST, W. T. 2008 A spatially developing one-dimensional turbulence (ODT) study of soot and enthalpy evolution in meter-scale buoyant turbulent flames. *Combust. Sci. Tech.* Submitted.